Rev. Roum. Sci. Techn.– Électrotechn. et Énerg.
Vol. **69**, *2*, pp. 207–212, Bucarest, 2024

ENHANCEMENT RIPPLES OF A DIRECT TORQUE CONTROL APPLIED TO A PERMANENT MAGNET SYNCHRONOUS MOTOR BY USING A FOUR-LEVEL MULTICELLULAR INVERTER AND A NEW REDUCED SWITCHING TABLE

BACHIR MOKHTARI

Keywords: Conventional switching table (CST); Direct torque control (DTC); Four-level multicellular inverter (4LMI); Permanent magnet synchronous motor (PMSM); Reduced switching table (RST).

The improvement of the direct control of flux and torque (DTC) essentially consists of reducing the ripples encountered at the levels of the torque and the stator magnetic flux. This control technique is widely used in various applications that recently employ the permanent magnet synchronous motor (PMSM). The improvement techniques are grouped into two large families: those that use multilevel inverters and require an additional cost to the driven system, which is only encouraging if the application covers this cost, and those that offer selection tables. This last solution is advantageous because it does not need any added device. In this paper, we propose to combine the two solutions, using a reduced switching table (RST) compared to the conventional switching table (CST) and using a four-level multicellular inverter (4LMI). This solution brought very satisfactory results by significantly reducing the ripples.

1. INTRODUCTION

Research to improve electric motors' direct flux and torque control (DTC) technique hardly ceases in the field of study and development. This technique, known in the 1980s, is classified among vector control techniques; credit goes to me. Takahashi and his team and after him to M. Depenbrock, for first introducing the technique to the applied academic and industrial spaces [1,2]. All techniques encounter problems that limit their performances, and it is up to researchers to find the appropriate solutions to remedy these problems and thus improve their robustness.

As for the DTC, the motor's ripples of flux and torque, when driven by DTC, mark its major drawback [3,4]. Several studies have then appeared to reduce these ripples; they can be classified into two large groups: the first concerns techniques based on the control model of the hysteresis bands [4-6] or the modified switching tables [7–17] and the second is based on the use of devices having the possibility of providing more vector-voltage to refine the controlled quantities or those applied to a dual star motor combined with the technics AI [18–26].

Finding a solution among the first group is very beneficial because it does not impose an additional cost on the system. Still, sometimes, the requested improvement requires combining those two improvement groups.

In this work, we propose two tricks to improve the DTC applied to drive a permanent magnet synchronous motor (PMSM): the first is to use a four-level multicellular inverter (4LMI) to ensure a greater number of vector voltages feed the motor, and the second is to use a reduced switching table (RST), whether in the case of conventional DTC or 4LMI.

The work is structured according to the following plan: first, the model of the system studied under the Simulink/ MATLAB environment, in which CST and RST are tested and validated experimentally on the testbed used in [10]; second, the reduced switching tables and the 4LMI; and third, the results obtained and their discussion. At the end, a conclusion and perspectives of this study will be given.

2. MODELING OF THE SYSTEM

The driven motor is a three-phase synchronous motor with a rotor consisting of a permanent magnet (PMSM). In a conventional DTC, the motor is powered by a two-level three-phase inverter. The control of this inverter allows the control of the motor; we impose pulses generated according to the conventional switching table (CST) presented for the first time by [1] and applied to an induction motor. To apply the DTC control to the PMSM, it is appropriate to choose the motor model between several models; the chosen model is presented in Fig. 1.

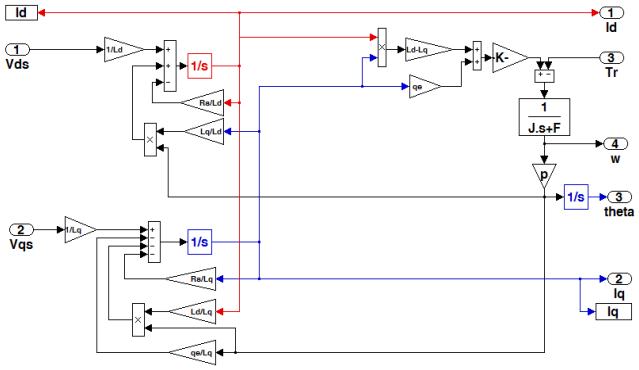

Fig. 1 – Model adopted for the PMSM.

The stator flux is estimated using expression (1), which shows that this estimate depends only on a single motor parameter: the stator resistance [5].

$$\begin{cases} \psi_{s\alpha} = \int (v_{s\alpha} - R_s i_{s\alpha}) \mathrm{d}t\,, \\ \psi_{s\beta} = \int (v_{s\beta} - R_s i_{s\beta}) \mathrm{d}t, \\ |\psi_s| = \sqrt{\psi_{s\alpha}^2 + \psi_{s\beta}^2}. \end{cases} \quad (1)$$

Its position is estimated after calculating the two components of the stator flux [5]:

$$\theta = \operatorname{atan} \frac{\psi_{s\beta}}{\psi_{s\alpha}}. \quad (2)$$

Faculty of Technology, University of Laghouat, 37G Ghardaia Road, 03000, Algeria. E-mail: ba.mokhtari@lagh-univ.dz / mokhtari71@yahoo.fr

DOI: 10.59277/RRST-EE.2024.69.2.15

Both stator currents need to be measured, and with the two stator flux components already estimated, the mechanical torque can be estimated using [5]:

$$T_m = \frac{3}{2} p\left(\psi_{s\alpha} i_{s\beta} - \psi_{s\beta} i_{s\alpha}\right). \quad (3)$$

3. REDUCED SWITCHING TABLE DEVELOPED AND THE 4MLI

The RST was first proposed by [10] and validated experimentally on DSP1103 for an asynchronous motor supplied by a two-level inverter. Subsequently, [27] studied its impact on the switching frequency and proved that it reduces it remarkably. These results confirm the study of [28].

The CST can be found in most references in this article; we are only interested in presenting the RST here. Table 1 presents the RST principle of application.

Table 1

Reduced switching table

	$\Delta\psi_S$	S_1	S_2	S_3	S_4	S_5	S_6	LINES
Ω<0	↓	001	101	100	110	010	011	1
	↑	101	100	110	010	011	001	2
Ω>0	↓	010	011	001	101	100	110	3
	↑	110	010	011	001	101	100	4

Here $\Delta\psi_S$ is the gap between the flux and its reference; S_1 is the first sector, between –30° and 30°, and 001 is the state of the half-arms of the inverter (0 for ON and 1 for OFF).

In a positive direction of rotation, only the vector voltages that increase the torque are used; in this case, the table with six lines becomes only two.

Condition (4) controls the torque linked to the speed sign and the fluctuation limit chosen beforehand.

The two remaining lines reverse the speed direction, reducing the torque. This ensures operation in quadrants 1 and 4, where operation is motor. The principle of RST is schematized according to the four quadrants in Fig. 2.

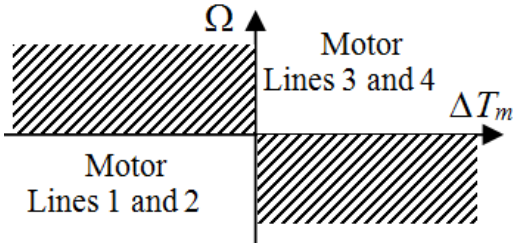

Fig. 2 – The condition to apply the RST.

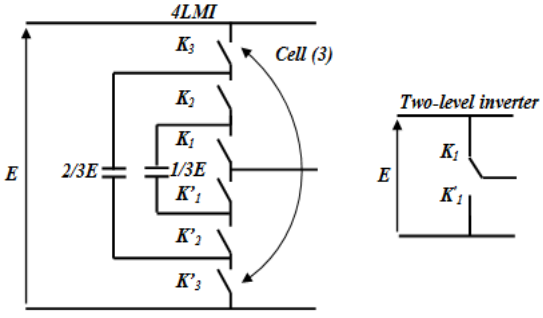

Fig. 3 – Presentation of one arm for the two-level inverter and that of 4LMI.

We now apply it to control the PMSM. Then, the basic two-level inverter will be replaced with another 4LMI whose CST is proposed by [28] (see Table 2). One arm of this inverter is presented with the arm of the conventional inverter two-level in Fig. 3.

For the 4LMI, there are 9 sectors, each with 40°. The vectors-voltages that the 4LMI can develop are presented in Fig. 4 [28].

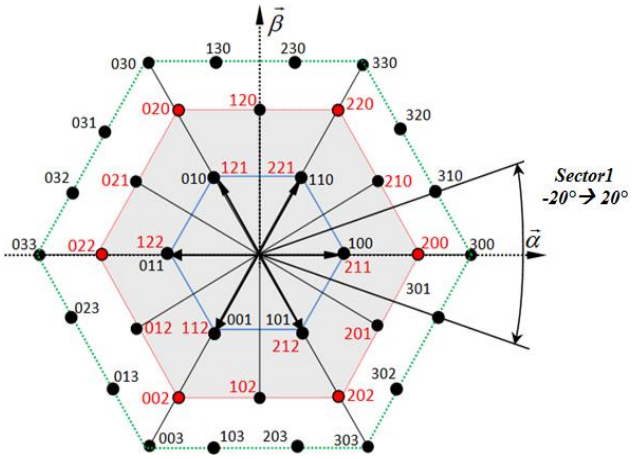

Fig. 4 – Space vector diagram of the 4LMI.

In several existing works like [20], the authors propose several tables suitable for each case of operation motor, but this one is unique and valid for any motor operation. This table is a bit bulky, so we propose reducing it using the same principle as [10].

For the 4LMI, this is a large switching table; the idea is to use only its half (for a given direction of rotation); on the one hand, we reduce this switching table, and on the other hand, we reduce the fluctuations of the electromagnetic torque and the magnetic flux of the stator.

The criterion that limits the use of this or that half of the switching table is determined by (4) [10],

$$\text{sign}(\Omega)\Delta T_m \leq 0. \quad (4)$$

When this condition is met, only zero voltage is applied. If the speed has only one direction of rotation, half of the CST becomes unusable, and we can eliminate it, for example, for an application that requires only one direction of rotation.

Table 2

Switching table for 4LMI

$\Delta\psi_S$	ΔT_m	S_1	S_2	S_3	S_4	S_5	S_6	S_7	S_8	S_9	Ω	
1↑	3↑⇑	330	130	031	033	013	103	303	301	310	+	
	2⇑	320	230	030	032	023	003	203	302	300		
	1↑	310	330	130	031	033	013	103	303	301		
	-3↓⇓	303	301	310	330	130	031	033	013	103		-
	-2⇓	302	300	320	230	030	032	023	003	203		
	-1↓	301	310	330	130	031	033	013	103	303		
	0	200	320	230	020	032	023	002	203	302		
0	3↑⇑	120	020	032	012	103	203	302	301	330	+	
	2⇑	120	020	032	012	103	203	302	301	330		
	1↑	120	020	032	012	103	203	302	301	330		
	-3↓⇓	102	202	301	210	230	130	031	023	003		-
	-2⇓	102	202	301	210	230	130	031	023	003		
	-1↓	102	202	301	210	230	130	031	023	003		
	0	000	000	000	000	000	000	000	000	000		
-1↓	3↑⇑	030	032	023	003	203	302	300	320	230	+	
	2⇑	031	033	013	103	303	301	310	330	130		
	1↑	021	012	002	203	302	200	320	230	020		
	-3↓⇓	003	203	302	300	320	230	030	032	023		-
	-2⇓	013	103	303	301	310	330	130	031	033		
	-1↓	002	203	302	200	320	230	020	021	012		
	0	122	013	103	212	301	310	221	130	031		

This condition linked to the sign of the speed selects only the lines of the CST, where the sign of the torque variation is that of the speed. Therefore, if the speed is positive, only the lines of the positive torque variation are used, and when it is negative, only those of the negative variations are used, as shown in Table 2.

For $\Omega > 0$ the CST can be reduced to the Table 3, and for $\Omega < 0$ only the rest of CST is used.

Table 3

RST for the 4LMI ($\Omega > 0$)

$\Delta\psi_s$	ΔT_m	S_1	S_2	S_3	S_4	S_5	S_6	S_7	S_8	S_9
1↑	3↑⇑	330	130	031	033	013	103	303	301	310
	2⇑	320	230	030	032	023	003	203	302	300
	1↑	310	330	130	031	033	013	103	303	301
0	3↑⇑	120	020	032	012	103	203	302	301	330
	2⇑	120	020	032	012	103	203	302	301	330
	1↑	120	020	032	012	103	203	302	301	330
-1↓	3↑⇑	030	032	023	003	203	302	300	320	230
	2⇑	031	033	013	103	303	301	310	330	130
	1↑	021	012	002	203	302	200	320	230	020

It is interest to know the dimensions of the four switching tables, RST are minimized than CST, like seen in Table 4.

Table 4

Dimensions of the four switching tables

	CST	RST	4LMI-CST	4LMI-RST
Lines	5	2 (for one speed direction)	21	9 (for one speed direction)
Columns	6		9	

DTC relies on the use of hysteresis bands to normalize the torque deviation from its reference and the flux deviation from its reference [1,2,4,6]. These hysteresis bands have an important impact on the ripples on flux and torque [3–6]. The levels of these bands used by this study for the CST and the RST for the two inverters are given in Table 5.

Table 5

Levels of hysteresis bands using for the two inverters

	Flux	Torque	
	CST or RST	CST	RST
DTC	2 levels (0,1)	3 levels (-1,0,1)	2 levels (0,1)
4LMI	3 levels (-1,0,1)	7 levels (-3,-2,-1,0,1,2,3)	4 levels (0,1,2,3) → for $\Omega > 0$ (0,–1,–2,–3) → for $\Omega < 0$

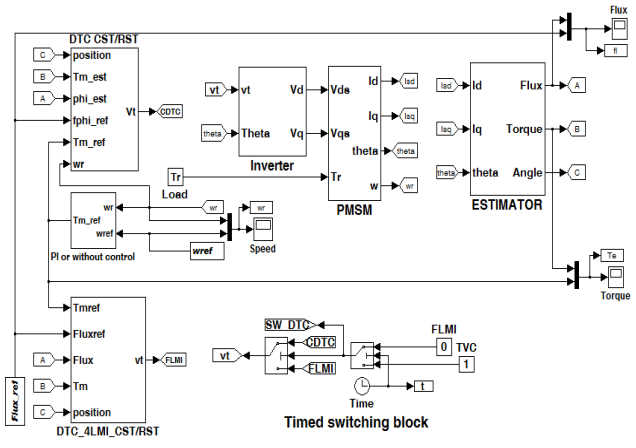

Fig. 5 – Diagram of all DTC techniques under Simulink/MATLAB.

The block diagram of the DTC control of the two inverters with the two switching tables is as illustrate by Fig. 5.

4. RESULTS ACHIEVED BY THIS STUDY

All the motor parameters necessary for the study are given in Table 6.

Table 6

PMSM parameters

Pole pairs	4
Stator resistance (Ω)	1.09
Stator inductance (Ld; Lq) (H)	0.0124
Permanent magnet flux (Wb)	0.1821
Inertia (kg.m²)	4.15×10^{-4}

While Table 7 presents the hysteresis bands chosen for this study. For the DTC with CST or RST, the magnetic flux has two levels, and the torque has three levels, while in the case of 4LMI they have three levels and seven levels respectively.

Table 7

Hysteresis bands chosen for magnetic flux and electromagnetic torque (S.I)

	Flux	Torque
DTC: CST/RST	0	3×10^{-5}
4LMI: CST/RST	10^{-3}	3: 3×10^{-5} 2: 1.5×10^{-5} 1: 7.5×10^{-5}

What interests us in this study is to show the improvement obtained by the proposed techniques. For this, we have adopted several simulations that can demonstrate the effectiveness of the study. The quantities that interest us are the electromagnetic torque, the magnetic flux and the stator current.

The switch block provides precise timing to switch between chosen techniques. We fixed the switching time so that each technique works within 0.1 s. The results obtained in this case are cited below.

The voltage vectors for the two inverters are illustrated in the following figures: this result confirms the inverters theory. The voltage vectors of 4LMI are numerous than those of the two-level inverter, this is confirmed by the presentation of Fig. 6.

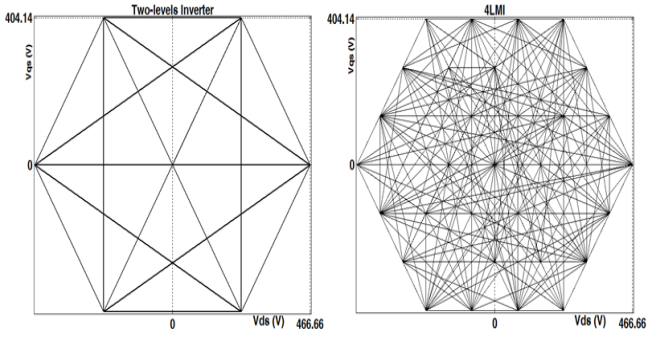

Fig. 6 – Space vector diagram of the two inverters voltage.

Figure 7 of the torque evolution shows an improvement and reduction in torque ripples, especially when RST is used.

However, the flow in Fig. 8 is slightly improved using RST, but its ripples are significantly reduced using 4LMI.

Visually, we cannot distinguish the best between them, so we need to examine the results further.

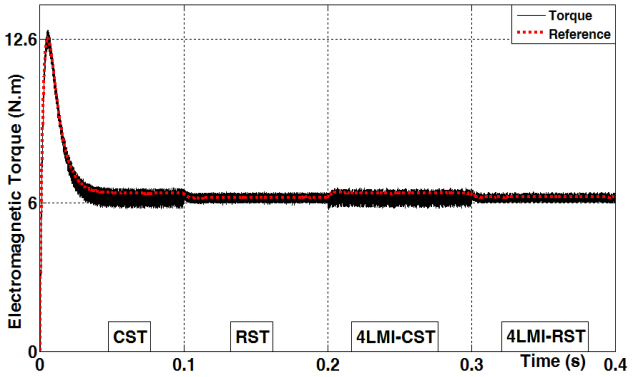

Fig. 7 – Torque evolution in the four cases of study.

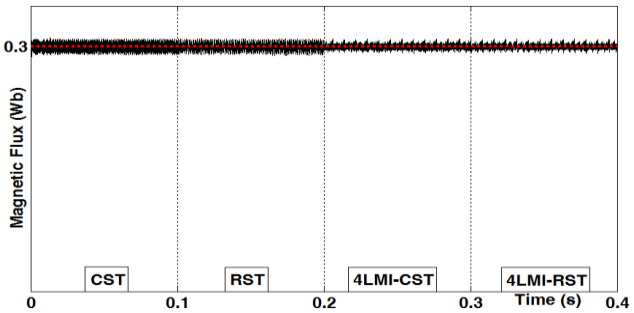

Fig. 8 – Flux amplitude evolution in the four cases of study.

We use the Data Statistic to calculate the peak-to-peak torque and flux for all cases, then compare them and plot the resulting values. The result obtained is presented in Table 8.

Table 8

Torque and flux ripples obtained by peak-to-peak calculation

	CST	RST	4LMI_CST	4LMI_RST
Torque ripple	0.8125 (100%)	0.5257 (64.7%)	0.7911 (97.36%)	0.4104 (50.51%)
Flux ripple	0.007691 (100%)	0.007579 (98.54%)	0.006735 (87.57%)	0.00653 (84.90%)

Figure 9 shows that using a 4LMI inverter with an RST switching table is the best choice because it improves by reducing torque and flux ripples together.

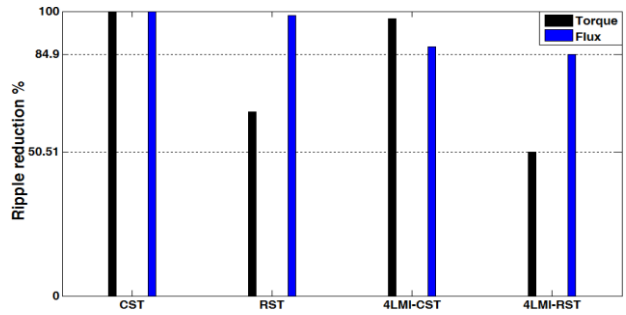

Fig. 9 – Torque and flux ripples reduction percent for all study cases.

It is now very interesting to see the effect of these configurations on the intensity of absorbed stator current. Figure 10 shows the current evolution for a single stator phase for all configurations.

These results note a good improvement obtained when using a 4LMI associated with the RST. We show this improvement in the following simulation, which only groups the DTC-CST and 4LMI-RST.

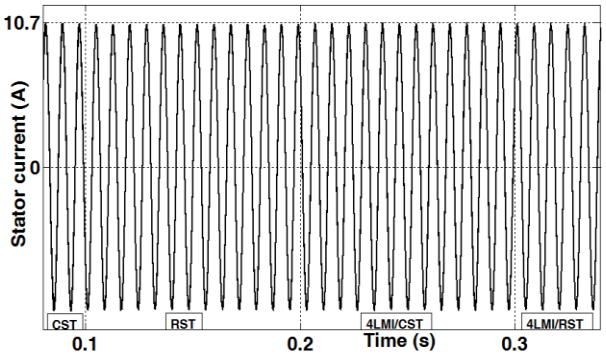

Fig. 10 – Stator current for one phase in all study cases.

Figure 11 illustrates the sector occupied by the flux vector for the two inverters when switching from DTC-CST to 4LMI-CST; we use the timed switch to toggle from DTC-CST to 4LMI-RST at t = 0.1 s. In the case of DTC with a two-level inverter (CST or RST), the flux vector occupies sectors 1 to 6, while in 4LMI (CST or RST), the number of sectors is 9.

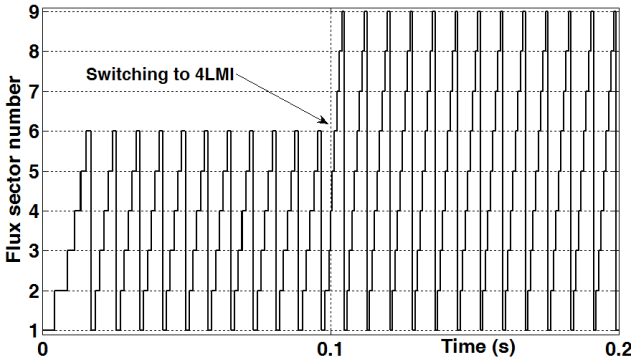

Fig. 11 – Sectors occupied by stator flux in simple DTC and 4LMI.

Figure 12 shows that the 4LMI-RST significantly reduces torque ripples. 50 % is a very important reduced value because torque ripples cause many operating problems for the system and health problems for the user.

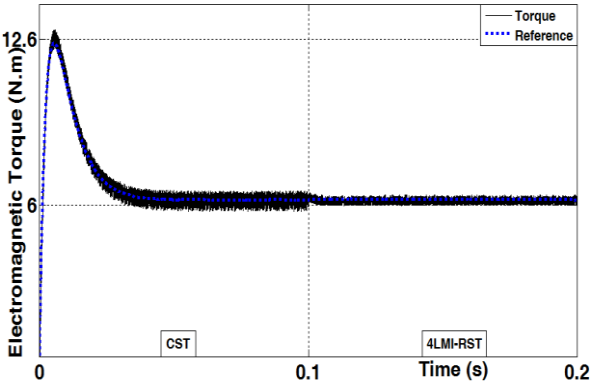

Fig. 12 – Evolution of the torque started by DTC-CST and switched to 4MLI-RST at t = 0.1 s.

In the same context, the flux in Fig. 13 shows less fluctuation using 4LMI-RST. The two famous flux trajectories in Fig. 14 show this significant reduction.

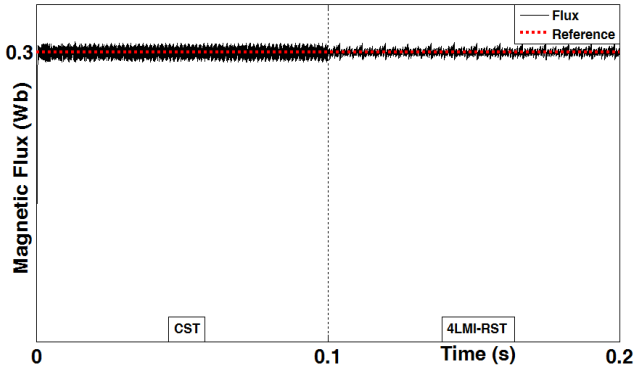

Fig. 13 – Evolution of flux amplitude started by DTC-CST and switched to 4MLI-RST at t = 0.1 s.

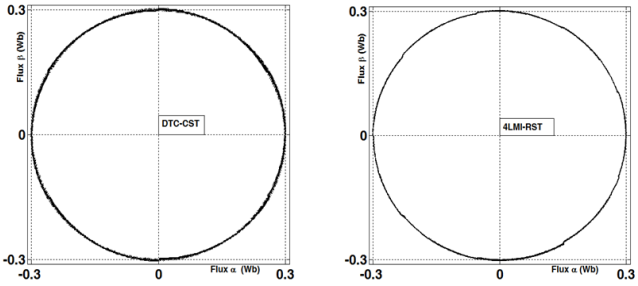

Fig. 14 – Stator flux trajectories in DTC-CST and 4LMI-RST.

5. **CONCLUSIONS**

This paper presents three solutions to reduce the torque and stator magnetic flux ripples of a PMSM driven by the DTC technique. The first solution uses the RST, a reduced switching table proposed by [10], which suitably reduces the fluctuations of the torque but little of those of the flux. The second solution is to use a four-level multicellular inverter (4LMI) to apply enough vector voltages to the motor. a suitable table for this inverter, which works perfectly in all conditions, has been presented. An improvement of the two fluctuations was obtained but needed to be more. The third solution presented is to assemble the two solutions and create an RST suitable for 4LMI. This solution attenuated the processed fluctuations (50.51 % for torque and 84.9 % for flux), greatly improving DTC's PMSM control. Following this work, we suggest a detailed study on harmonics created for each case previously studied and compare the switching frequency of each inverter (associated with the two switching tables).

Received on 26 July 2023

REFERENCES

1. I. Takahashi, T. Noguchi, *A new quick-response and high-efficiency control strategy of an induction motor*, IEEE Trans. Ind. Appl. IA, **22**, *5*, pp. 820–827 (1986).
2. M. Depenbrock, *Direct self-control (DSC) of inverter-fed induction machine*, IEEE Transactions on Power Electronics, **3**, *4*, pp. 420–429 (1988).
3. A.T. Siti Azura, J. Auzani, M.J. Mohd Luqman, A.K. Kasrul, S. Tole, *A review of direct torque control development in various multilevel inverter applications*, International Journal of Power Electronics and Drive System (IJPEDS), **11**, *3*, pp. 1675–1688 (2020).
4. J.K. Kang, D.W. Chung and S.K. Sul, *Direct torque control of induction machine with variable amplitude control of flux and torque hysteresis bands*, IEEE International Electric Machines and Drives Conference (IEMDC'99), Proceedings (Cat. No.99EX272), Seattle, WA, USA, 1999, pp. 640–642.
5. S.S. Hakami, K.B. Lee, *four-level hysteresis-based DTC for torque capability improvement of IPMSM fed by three-level NPC inverter*, Electronics, **9**, *10*, p. 1558 (2020).
6. P.S. Borse, M.P. Thakre, R. Shriwastava, *Employment of torque-hysteresis controller for DTC based induction motor drive*, Journal of Physics: Conference Series, **2062**, *1*, p. 012020 (2021).
7. C.A. Martins, X. Roboam, T.A. Meynard, A.S. Carvalho, *Switching frequency imposition and ripple reduction in DTC drives by using a multilevel converter*, IEEE Transactions on Power Electronics, **17**, *2*, pp. 286–297 (2002).
8. N.R.N. Idris, A.H.M. Yatim, *Direct torque control of induction machines with constant switching frequency and reduced torque ripple*, IEEE Transactions on Industrial Electronics, **514**, pp. 758–767 (2004).
9. B. Mokhtari, A. Ameur, L. Mokrani, B. Azoui, M.F. Benkhoris, *Comparative experimental study of three switching tables of a DTC applied to an induction motor for a tracking system*, Journal of Electrical Engineering, **12**, *3*, 2012 (last accessed August 2023) – http://www.jee.ro/index.php/jee/article/view/WC1320233051W4eb1285b96770.
10. B. Mokhtari, M.F. Benkhoris, *High ripples reduction in DTC of induction motor by using a new reduced switching table*, Journal of Electrical Engineering, **67**, *3*, pp. 206–211 (2016).
11. F. Ramirez, M. Pacas, *Enhanced control of the torque ripple in a PMSM drive with variable switching frequency*, 19th European Conference on Power Electronics and Applications (EPE'17 ECCE Europe), Poland, 2017, pp. P.1–P.10.
12. J. Zhang, L. Li, D. Dorrell, Y. Guo, *Direct torque control with a modified switching table for a direct matrix converter-based ac motor drive system*, 20th International Conference on Electrical Machines and Systems (ICEMS), Sydney, NSW, Australia, 2017, pp. 1–6.
13. S.V. Bhangale, R. Kumar, K. Bhangale, *18-sector direct torque-controlled strategy with improved stator flux estimator for induction motor drive*, 8th IEEE India International Conference on Power Electronics (IICPE), Jaipur, India, pp. 1–6, 2018.
14. R.E. Kodumur Meesala, V.K. Thippiripati, *An improved direct torque control of three-level dual inverter fed open-ended winding induction motor drive based on modified look-up table*, IEEE Transactions on Power Electronics, **35**, *4*, pp. 3906–3917 (2020).
15. F. Yashar, M. Alzayed, H. Chaoui, S. Kelouwani, *A novel switching table for a modified three-level inverter-fed DTC drive with torque and flux ripple minimization*, Energies, **13**, *18*, p. 4646 (2020).
16. B.D. Lemma, S. Pradabane, *Control of PMSM drive using lookup table based compensated duty ratio optimized direct torque control (DTC)*, IEEE Access, **11**, pp. 19863–19875 (2023).
17. M.M. Alshbib, I.M. Alsofyani, M.M. Elgbaily, *Enhancement and performance analysis for modified 12 sector-based direct torque control of ac motors: Experimental Validation*, Electronics, **12**, *3*, p. 549 (2023).
18. M.F. Escalante, J.C. Vannier, A. Arzande, *Flying capacitor multilevel inverters and DTC motor drive applications*, IEEE Transactions on Industrial Electronics, **49**, *4*, pp. 809–815 (2002).
19. K.B. Lee, J.H. Song, I. Choy, J.Y. Yoo, *Torque ripple reduction in DTC of induction motor driven by three-level inverter with low switching frequency*, IEEE Transactions on Power Electronics, **17**, *2*, pp. 255–264 (2002).
20. A. Tlemçani, *Contribution to the Application of Adaptive Controls by Fuzzy Systems to a Synchronous Machine with Permanent Magnets Fed by a Serial Multicellular Converter, (Contribution à l'Application des Commandes Adaptatives par les Systèmes Flous à une Machine Synchrone à Aimants Permanents Alimentée par un Convertisseur Multicellulaire Série)*, Dissertation, National Polytechnic School, Algeria, 2007 (last accessed August 2023) https://repository.enp.edu.dz/xmlui/handle/123456789/382
21. F. Khoucha, S.M. Lagoun, K. Marouani, A. Kheloui, M.E.H. Benbouzid, *Hybrid Cascaded H-bridge multilevel-inverter induction-motor-drive direct torque control for automotive applications*, IEEE Transactions on Industrial Electronics, **57**, *3*, pp. 892–899 (2010).
22. H. Sudheer, S.F. Kodad, B. Sarvesh, *Improvements in direct torque control of induction motor for wide range of speed operation using fuzzy logic*, Journal of Electrical Systems and Information Technology, **5**, *3*, pp. 813–828 (2018).
23. B.R. Vinod, G. Shiny, *Direct torque control scheme for a four-level-inverter fed open-end-winding induction motor*, IEEE Transactions on Energy Conversion, **34**, *4*, pp. 2209–2217 (2019).

24. R. Belal, M. Flitti, M.L. Zegai, *Tuning of PI speed controller in direct torque control of dual star induction motor based on genetic algorithms and neuro-fuzzy schemes*, Rev. Roum. Sci. Techn. – Électrotechn. et Énerg., **69**, *1*, pp. 9–14 (2024).
25. E. Benyoussef, S. Barkat, *Direct torque control based on space vector modulation with balancing strategy of dual star induction motor*, Rev. Roum. Sci. Techn. – Électrotechn. et Énerg., **67**, *1*, pp. 15–20 (2022).
26. A. Derbane, B. Tabbache, A. Ahriche, *A fuzzy logic approach based direct torque control and five-leg voltage source inverter for electric vehicle powertrains*, Rev. Roum. Sci. Techn. – Électrotechn. et Énerg., **66**, *1*, pp. 9–14 (2021).
27. K. Lv, Z. Xie, M. Zhou, J. Bu, *A comparative study of three starting strategies for an aero flywheel motor using the modified DTC method*, IEEE Access, **7**, pp. 59548–59558 (2019).
28. B. Mokhtari, *Intelligent DTC Applied to the Control of the Asynchronous Machine, (DTC Intelligence Appliquée à la Commande de la Machine Asynchrone)*, Dissertation, University of Batna2, Algeria, 2014 (last accessed August, 2023) – http://eprints.univ-batna2.dz/1244/1/ing Bachir Mokhtari.pdf